analytical chemistry

ARTICLE

pubs.acs.org/ac

Manganese-Doped ZnSe Quantum Dots as a Probe for Time-Resolved Fluorescence Detection of 5-Fluorouracil

Dong Zhu,[†,‡] Yun Chen,[†] Liping Jiang,[†] Jun Geng,[†] Jianrong Zhang,[*,†] and Jun-Jie Zhu[*,†]

[†]State Key Laboratory of Analytical Chemistry for Life Science, School of Chemistry and Chemical Engineering, Nanjing University, Nanjing 210093, People's Republic of China

[‡]College of Pharmacy, Nanjing University of Chinese Medicine, Nanjing 210046, People's Republic of China

Supporting Information

ABSTRACT: Quantum dots (QDs) are generally used for the conventional fluorescence detection. However, it is difficult for the QDs to be applied in time-resolved fluorometry due to their short-lived emission. In this paper, high-quality Mn-doped ZnSe QDs with long-lived emission were prepared using a green and rapid microwave-assisted synthetic approach in aqueous solution. Fluorescence lifetime of the Mn-doped ZnSe QDs was extended as long as 400 μs, which was 10 000 times higher than that of conventional QDs such as CdS, CdSe, and CdTe. The QDs exhibited an excellent photostability over 35 h under continuous irradiation at 260 nm. Capped with mercaptopropionic acid (MPA), the Mn-doped ZnSe QDs were used for the time-resolved fluorescence detection of 5-fluorouracil (5-FU) with the detection limit of 128 nM. The relative standard deviation for seven independent measurements of 1.5 μM 5-FU was 3.8%, and the recovery ranged from 93% to 106%. The results revealed that the Mn-doped ZnSe QDs could be a good candidate as a luminescence probe for highly sensitive time-resolved fluorometry.

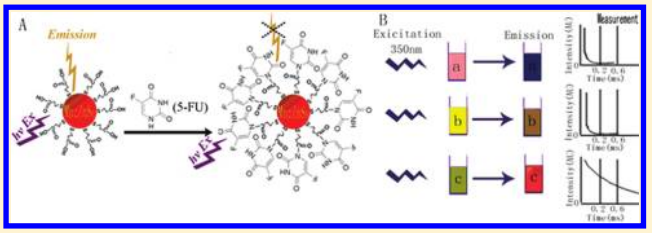

Time-resolved fluorometry has become a valuable tool for the determination of antigens, antibodies, proteins, peptides, and oligonucleotides.[1,2] It can effectively eliminate short-lived scattering light and background noise from the specific fluorescence signal of the long-lived fluorescence probe, which results in the high sensitivity and wide dynamic range. At present, the probes for time-resolved fluorometry were mainly lanthanide chelates owing to their long fluorescence lifetime (as long as 20−1000 μs), large Stoke's shift, and narrow emission peaks. However, the luminescence of the lanthanide chelates is weaker than that of organic fluorescent dyes due to lower luminescence quantum yields and smaller molar extinction coefficients of the chelates. Also, photobleaching is serious for lanthanide chelate probes in the monitoring of some real-time biological processes such as luminescence bioimaging.[3] Development of a fluorescent probe with stronger luminescence and better photostability is critical for the further application of time-resolved fluorometry in biological study.

Quantum dots (QDs) have emerged as the attractive fluorescent probes for biological detection and biotechnology, mainly due to their unique luminescent quality such as strong photoluminescence and good photostability.[4−9] Cadmium chalcogenide QDs are widely explored. However, their fluorescence lifetime is similar to that of the background autofluorescence, which obstructs the application of these traditional QDs in the time-resolved fluorometry. In addition, cadmium chalcogenide QDs are toxic to the biological system and sensitive to heat, chemical, and photochemical disturbances, which limits the QDs as biomedical probes.[10−16] Manganese ion (Mn^{2+})-doped QDs especially using ZnSe or ZnS as the hosts are a novel class of luminescent materials, which retain some advantages of the conventional QDs and offer significant solution to the above problems.[17,18] In the semiconductor nanocrystal lattices, the doping ions Mn^{2+} substitute for the cations Zn^{2+} and act as a luminescence center resulting in strong and characteristic emission due to the $^4T_1(^4G) \rightarrow {}^6A_1(^6S)$ transition of the Mn^{2+}.[19] Its photoluminescence (PL) is much higher than that of the bulk counterpart. Moreover, the emission has excellent thermal, chemical, and photochemical stabilities, which are attributed to the nature of the atomic-like emission states.[23,25] Most importantly, the fluorescence lifetime of the Mn^{2+} emission was observed to be as long as hundreds of microseconds according to recent reports.[30,31] Yan's group[20] has acquired pioneering progress in the field of time-resolved photoluminescence analysis using QDs as a probe. They used the Mn-doped ZnS QDs as a room-temperature phosphorescence (this is also time-resolved photoluminescence mode) probe for the facile, cost-effective, sensitive, and selective detection of enoxacin for the first time in 2008.[20a] Subsequently, the Mn-doped ZnS QDs have been explored to detect DNA,[20b] pentachlorophenol,[20c] glucose,[20d] ascorbic acid,[20e] 2,4,6-trinitrotoluene (TNT),[20f] and protein.[20g] The method allowed the detection without interference from autofluorescence and the scattering light of the matrix. However, some reports[21,22] indicated that a large amount of surface defects

Received: August 10, 2011
Accepted: October 26, 2011
Published: October 26, 2011

that existed in the Mn-doped ZnS QDs could serve as nonradiative recombination paths for the excitation energy, which would quench the emission of Mn^{2+} to some extent, and this would make sensitivity of detection decrease. Until now, the use of the QDs for time-resolved optical sensing is only on its infant stage but has proven to be very promising.[20e]

Lately, Norris's and Peng's groups found the Mn-doped ZnSe QDs could exhibit better optical performance such as stronger photoluminescence and better photostability.[24,25] Various methods have been developed to synthesize the Mn-doped ZnSe QDs. In 2001, Norris et al.[24] first presented an organometallic route for the preparation of the Mn-doped ZnSe QDs, which confirmed that the Mn^{2+} was embedded inside the nanocrystals. Peng and co-workers[23,25] introduced nucleation-doping and growth-doping synthetic strategies in the high-temperature organometallic synthesis. Recently, a microwave-assisted hydrothermal procedure was used for the synthesis of various nanomaterials.[26−28] It exhibited many distinct advantages over conventional synthesis in aqueous solution such as rapid heating to crystallization temperature, fast supersaturating by the rapid dissolution of precipitated gels, and eventually a shorter crystallization time compared with conventional external heating. In our recent communication,[29] a green and rapid synthetic procedure was presented for the synthesis of the Mn-doped ZnSe/ZnS core/shell QDs in aqueous phase by microwave irradiation.

In this paper, the low-toxic Mn-doped ZnSe QDs (Mn-QDs) were synthesized following our previous report.[29] It was observed that the Mn-QDs had long fluorescence lifetime, close to that of the lanthanide chelates, and high photoluminescence stability. A time-resolved fluorometry was demonstrated to determine 5-fluorouracil (5-FU) in human serum PBS solution using the Mn-QDs as the fluorescence probe. 5-FU has widely been used in the treatment of various cancers including the breast, pancreas, stomach, and rectum cancer.[34] An enhancement of detectable accuracy was obtained, which was attributed to the elimination of the background fluorescence interference of 5-FU and human serum. The experimental results revealed that the Mn-QDs might be a new promising fluorescence probe for time-resolved fluorometry.

EXPERIMENTAL SECTION

Chemicals. 3-Mercaptopropionic acid (MPA, 99%) and 5-fluorouracil (5-FU) were from Fluka. $Zn(NO_3)_2$ (99%), $MnCl_2$ (99%), $NaBH_4$ (96%), sodium oleate (99%), and selenium powder (99.999%, about 200 mesh) were obtained from Shanghai Reagent Company. Ethanol (CH_3CH_2OH, anhydrous) was of analytical grade and used without further purification. Other chemicals were of analytical grade. Phosphate buffer solution (PBS, 25 mM, pH = 7.4) was prepared by mixing the solutions of K_2HPO_4 and NaH_2PO_4. Ultrapure water with 18.2 MΩ (Millipore Simplicity, U.S.A.) was used in the experiments. The serum samples were collected from healthy volunteers. No further pretreatment and deproteinization procedures were needed in the sample preparation.

Characterization. X-ray diffraction (XRD) measurements were performed on a Shimadzu XRD-6000 powder X-ray diffractometer, using Cu Kα (λ = 1.5405 Å) as the incident radiation. Inductively coupled plasma atomic emission spectroscopy (ICP-AES) was performed on a Perkin-Elmer Optima 3000 DV after dissolving the aqueous Mn-QDs in 5% hydrochloric acid. Transmission electron microscopy (TEM) and high-resolution TEM (HRTEM) samples were prepared by dropping the samples dispersed in water onto carbon-coated copper grids with excess solvent evaporated. TEM images were recorded on a Shimadzu JEM-2010 CX with an accelerating voltage of 100 kV. HRTEM images were recorded on a JEM-2010 F with an accelerating voltage of 200 kV. UV−vis absorption spectra were obtained using a UV-3600 spectrophotometer (Shimadzu). Fluorescence measurements were performed using a Shimadzu RF-5301 PC fluorescence spectrometer. The room-temperature photoluminescence quantum yield of the Mn-QDs was estimated following the ref 32 by using rhodamine 6G as a reference standard. Electron paramagnetic resonance (EPR) measurements were performed using an X-band (9.7747 GHz) EMX-10/12 spectrometer (Bruker) at room temperature. Cylindrical quartz tube containers were used to insert the powders into the microwave cavity. The fluorescence lifetime of the Mn-QDs was measured with a FLS 920 time-resolved spectroscope (Edinberge). The time-resolved fluorescence spectrum was performed on an LS-55 fluorometer (Perkin-Elmer). All of the measurements were performed at room temperature except the photostability measurement of the Mn-QDs at 37 °C.

Synthesis of the Mn-QDs. A microwave synthetic system (CEM Discover) was used for the preparation of the Mn-QDs. The reaction temperature, pressure, and time were programmed in the reaction. The synthesis of the Mn-QDs was performed in a high-strength cylindrical digestion vessel consisting of a special kind of glass. The volume of vessel used in the reaction was 80 mL. In a typical synthesis, 3.0 g of sodium oleate was added to the mixture of 15 mL of water and 5 mL of ethanol, and the pellucid solution was obtained by stirring intensively for 5 min. An amount of 10 mL of aqueous solution containing 0.25 g of zinc nitrate and 0.02 g of manganese chloride was added to the sodium oleate solution, which was stirred intensively for 5 min under nitrogen atmosphere. Then 5 mL of freshly prepared NaHSe solution was added to the above reaction mixture and stirred for 10 min under nitrogen atmosphere.[33] The molar ratio of Zn^{2+}/Se^{2-} was equal to 3:1. The mixture was transferred to an 80 mL cylindrical digestion vessel under agitation. Under microwave irradiation (260 W), the reaction was maintained at 170 °C and 175 psi for 40 min. In this procedure, metal ions (Zn^{2+}, Mn^{2+}) first underwent an ion-exchange process to form metal oleate. In the addition of Se^{2-} ion, the reaction between metal oleate and Se^{2-} generated metal selenide precursors, which were interacted to form Mn-QDs. Along with the process, the Mn-QDs were endowed with hydrophobic surfaces coated with the alkyl ligands of oleate. The spontaneous separation of the Mn-QDs from the bulky solution occurred due to the weight of the Mn-QDs and the incompatibility between the hydrophobic surface and their hydrophilic surrounding. The Mn-QDs that collected at the bottom of the container were redispersed in 50 mL of chloroform. After centrifugation at 10 000 rpm, the transparent upper Mn-QDs solution was collected. The solution was dried in vacuum, and the flaxen Mn-QDs powders of about 80 mg were obtained. The flaxen Mn-QDs coated with the original alkyl ligands were dissolved in 2 mL of chloroform and treated with 200 μL of MPA. The mixture was shaken for 60 min under sonication. The chloroform solution gradually became turbid because the original ligands with a long hydrophobic alkyl chain were replaced by the hydrophilic carboxyl chain of MPA. The MPA-coated Mn-QDs precipitate was isolated by centrifugation. Excess MPA was further removed by washing the precipitate with chloroform for three times. The final precipitate was

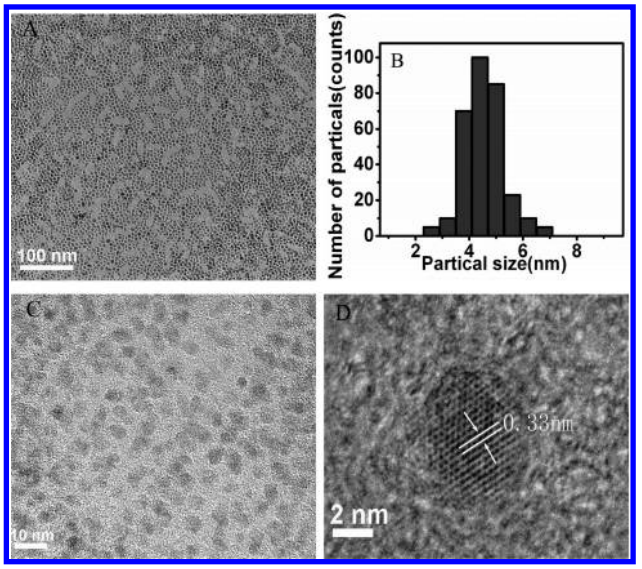

Figure 1. (A) TEM image of the Mn-QDs. (B) Particle size distribution histogram. The size distribution histogram was obtained by averaging the sizes of 150 particles from the TEM image. (C) HRTEM image of the Mn-QDs. (D) HRTEM image of one individual Mn-QD.

dried in vacuum, and the flaxen Mn-QDs powders were obtained. The powders can be dispersed to PBS solution (pH 7.4). The content of the incorporated Mn^{2+} in the Mn-QDs was determined by ICP-AES after dissolving the Mn-QDs in 5% hydrochloric acid solution. In the typical synthesis, the Mn/Zn mass ratio of 10% in the reaction solution gave the incorporated Mn^{2+} ratio of 0.84% in the prepared Mn-QDs.

Time-Resolved Fluorescence Detection of 5-FU. Amounts of 300 μL of 30 mg/L Mn-QDs solution, 300 μL of PBS solution (pH 7.4), and 200 μL of serum solution of 50-fold dilution containing given concentrations of 5-FU were sequentially added to a 1 mL calibrated test tube. The mixture was then diluted with PBS solution and mixed thoroughly. The time-resolved fluorescence measurements were carried out with the excitation wavelength of 350 nm, delay time of 0.2 ms, gate time of 0.4 ms, and cycle time of 20 ms in the absence or presence of a series of 5-FU solutions.

RESULTS AND DISCUSSION

Characterization of the Mn-QDs. The crystalline structure of the Mn-QDs was determined with XRD as shown in Figure S1A (see the Supporting Information). All of the XRD peaks of the Mn-QDs were indexed as the cubic zinc blende structure, which was consistent with the values in previous reports.[24,25] The incorporation of Mn^{2+} ions into the ZnSe nanocrystalline lattices was confirmed by EPR spectroscopy as shown in Supporting Information Figure S1B. The detailed experimental data and discussion are in the Supporting Information.

Figure 1 shows good monodispersity and high crystallinity of the Mn-QDs with particle sizes ranging from 4.5 to 5.5 nm. The HRTEM image of one individual Mn-QD in Figure 1D exhibited the distance between the adjacent lattice fringes to be 0.33 nm, which corresponded with the literature value for the (111) d spacing, 0.324 nm (JCPDF no. 800021).)

Water Solubilization of the Mn-QDs. The Mn-QDs capped with the alkyl chain were easily dispersed into chloroform to form

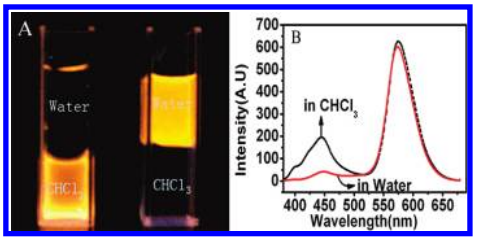

Figure 2. (A) Digital pictures of the Mn-QDs before (left) and after (right) ligand exchange under UV irradiation. (B) Dashed and solid lines are the PL spectra before (in $CHCl_3$) and after (in water) MPA ligand exchange, respectively. Excitation wavelength was 350 nm.

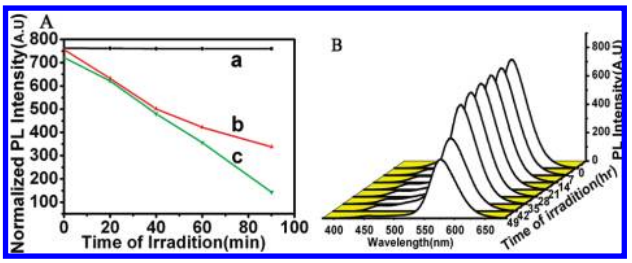

Figure 3. (A) Photostability comparison of the Mn-QDs, CdTe QDs, and fluorescein isothiocyanate (FITC) in water at 37 °C under continuous irradiation at 260 nm using a 150 W xenon lamp: (a) Mn-QDs, the optical density (OD) was 0.39; (b) CdTe QDs, the OD was 0.36; (c) FITC, 1.0×10^{-5} mol/L. (B) Photostability of the Mn-QDs in the same condition with panel A. The OD of the solution at 350 nm was 0.39.

a homogeneous solution. Replacing the long hydrophobic alkyl chains by the hydrophilic carboxyl chain of MPA caused the Mn-QDs to be dispersed into water. Figure 2A shows digital pictures of the Mn-QDs before (left) and after (right) ligand exchange under UV irradiation. In Figure 2B, the PL spectra exhibits two peaks. The orange peak around 585 nm came from an internal electronic transition of the Mn^{2+} ($^4T_1 \rightarrow {}^6A_1$), and the blue peak around 450 nm came from excitation recombination in the ZnSe. The surface ligand exchange could hardly quench the PL around 585 nm, although it could quench the ZnSe band-edge PL around 450 nm. The distinct difference of PL response was explained by the different emission mechanisms. When an intrinsic quantum dot was excited by photons with energy higher than its band gap, an excitation (an electron−hole pair) was generated. The direct recombination of the electron−hole pair caused the quantum dot to emit photons, typically being quantum-confined in the case of QDs,[34] and gave the well-known band-edge emission. However, the orange emission around 585 nm of Mn-QDs was different. The internal electronic transition of the Mn ($^4T_1 \rightarrow {}^6A_1$) led to the characteristic dopant emission around 585 nm from the Mn^{2+} ion. When the long hydrophobic alkyl chain was replaced by the hydrophilic carboxyl chain of MPA, the photogenerated holes in the Mn-QDs were trapped onto the thiol ligands of MPA on the Mn-QDs surface[25] and served as nonradiative recombination paths for the ZnSe electron−hole pair. And they induced the PL of the intrinsic ZnSe band edge to be quenched. However, the PL around 585 nm is inner electron states transition of the doping centers, which thus was not affected by the surface ligands. The PL quantum yield (QY) of the Mn-QDs was up to 16%.

Photostability of the Mn-QDs. Since the low-toxic Mn-QDs can be used as bioimaging agents in biomedical assay, their photostability is critical. Figure 3A shows the photostability of

the Mn-QDs, the conventional CdTe QDs reported in ref 35, and traditional organic fluorescent dye, fluorescein isothiocyanate (FITC). The PL intensity of the Mn-QDs remained almost constant during the whole 90 min in UV irradiation. However, the PL intensity of CdTe QDs and FITC decreased to 45% and 20% of the original PL intensity, respectively. The long-term investigation exhibited that the PL intensity of the Mn-QDs remained at 91% after 35 h and 54% after 49 h of irradiation, respectively, as shown in Figure 3B. The excellent photostability of Mn-QDs may be attributed to the nature of the internal electronic transition of the Mn ($^4T_1 \rightarrow {}^6A_1$) and noncoupling with the lattice phonons.

Application of the Mn-QDs for Time-Resolved Fluorometry. The fluorescence lifetime of the conventional QDs such as CdSe, CdTe, and CdS was several decades of nanoseconds, and that of the organic fluorescent dye was only a few nanoseconds.[36] The fluorescence lifetime of the Mn-QDs measured at the peak of 585 nm was as long as 400 μs, which was consistent with the values in previous reports,[30,31] as shown in Figure 4. It was close to the fluorescence lifetime of the lanthanide chelates, which was 20−1000 μs. The long fluorescence lifetime was propitious for the time-resolved fluorometry.

Time-resolved fluorometry was established to determine 5-FU in human serum PBS solution using the Mn-QDs as a probe. Figure 5A shows the schematic illustration of the time-resolved fluorometry. The carboxylic groups on the surface of MPA-capped Mn-QDs acted as the receptor sites to bind the −NH groups of 5-FU species. The binding of 5-FU onto the surface of the Mn-QDs was confirmed using infrared spectroscopy as shown in Supporting Information Figure S2, which can effectively quench the fluorescence intensity of the Mn-QDs.

Figure 5B illustrates fluorescence temporal selection of 5-FU, human serum, and the Mn-QDs. After the short-lived background fluorescence of both 5-FU and human serum disappeared by delaying the measuring time, the long-lived Mn-QDs fluorescence were then determined to effectively eliminate fluorescence interference of both 5-FU and human serum.

Figure 6A compares the fluorescence spectra of the Mn-QDs in human serum PBS solution containing 5-FU using conventional fluorometry and time-resolved fluorometry. In the conventional fluorescence spectra, the emissions of both 5-FU and human serum from 400 to 620 nm interfered with the emission peaks at 450 and 585 nm of the Mn-QDs (curves a−c in Figure 6A). The fluorescence interferences led to a serious limitation in analytical accuracy and testing sensitivity. However, in the time-resolved fluorescence spectra, the short-lived fluorescences of both 5-FU and human serum from 400 to 620 nm were disappeared by delaying the detection time, and thus, no fluorescence interference (curve d in Figure 6A) was observed. These experiments suggested that the Mn-QDs could be used as a time-resolved fluorescence probe to detect 5-FU. Figure 6B exhibits the PL quenching responses of 5-FU to the Mn-QDs. The PL quenching followed the Stern−Volmer equation:

$$P_0/P = 1 + K_{SV}c_q \quad (1)$$

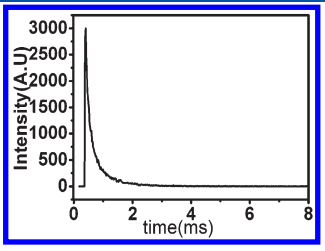

Figure 4. Photoluminescence decay of the Mn-QDs dispersed in PBS solution, pH 7.4. Excitation wavelength: 350 nm.

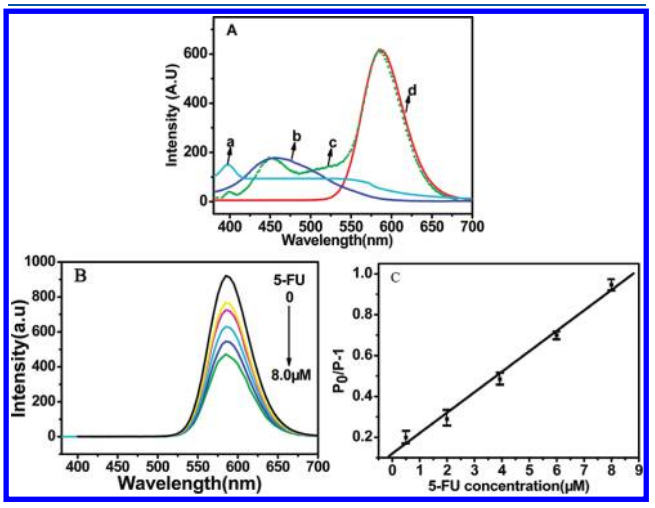

Figure 6. (A) Conventional fluorescence spectra of 5-FU (a), human serum (b), a mixture of 5-FU, Mn-QDs, and human serum (c), and time-resolved fluorescence spectra of the mixture (d) in PBS solution (pH = 7.4). (B) Time-resolved fluorescence spectra of the Mn-QDs with different 5-FU concentrations. (C) Calibration curve for 5-FU. Conventional fluorescence measurement condition: excitation wavelength, 350 nm. Time-resolved fluorescence measurement condition: excitation wavelength, 350 nm; delay time, 0.2 ms; gate time, 0.4 ms; cycle time, 20 ms. Error bars mean the standard deviation. Each point was an average value of three independent measurements.

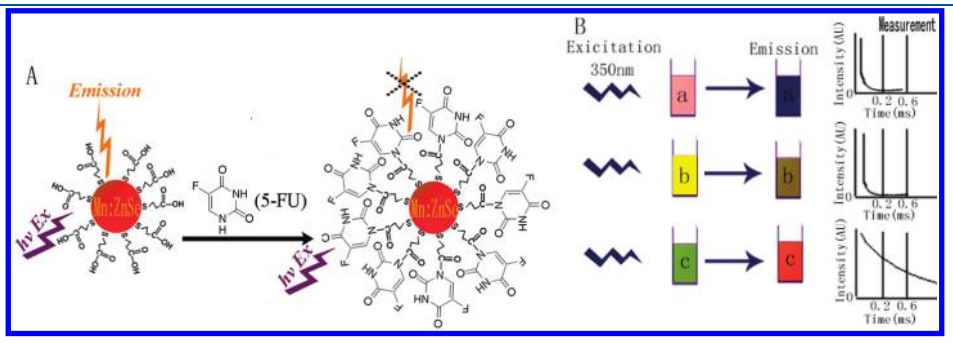

Figure 5. (A) Schematic illustrations of time-resolved fluorometry using the MPA-capped Mn-QDs as a fluorescence probe for 5-FU detection. (B) Fluorescence temporal selection of 5-FU (a), human serum (b), and the Mn-QDs (c).

dx.doi.org/10.1021/ac202101u |*Anal. Chem.* 2011, 83, 9076–9081

Table 1. Effect of Coexisting Substances on the Determination of 1.5 μM 5-FU

substance	concn (μM)	change in the determination (%)
Na^+	6000	+2.1
K^+	12000	+2.5
Ca^{2+}	12000	−4.5
Mg^{2+}	12000	+3.8
histidine	1200	−4.1
L-cysteine	1200	−3.9
glucose	12000	+3.0

Table 2. Recovery (Mean ± s; n = 3) for the Determination of 5-FU in Serum Samples

sample	spiked concn (μM)	recovery (%)
human serum	0.80	102 ± 5
human serum	1.60	95.2 ± 4.1
human serum	2.40	105 ± 5

where P_0 and P are the fluorescence intensities in the absence and presence of a quencher, respectively, c_q is the concentration of the quencher, and K_{SV} is the quenching constant of the quencher. Figure 6C shows a linear calibration plot of the quenched PL intensity against the concentration of 5-FU in the range of 0.5−8.0 μM with a correlation coefficient of 0.996. The precision for seven repeated measurements of 1.5 μM 5-FU was 3.8% (RSD), and the detection limit (3δ) was 128 nM.

The components that exist in human serum are complex, which mainly include electrolytes, carbohydrates, and biological macromolecules such as fattiness, albumen, and peptides. We selected some representative electrolyte ions involved, Na^+, K^+, Ca^{2+}, and Mg^{2+}, glucose, and some small biomolecules such as histidine and L-cysteine for the interference test. Table 1 shows the specificity of the Mn-QDs as the probe. The determination of 5-FU at 1.5 μM was unaffected by 4000-fold excess of Na^+, 8000-fold excesses of K^+, Ca^{2+}, Mg^{2+}, and glucose, and 800-fold excesses of histidine and L-cysteine. In order to investigate the influence of other biological macromolecules for the detection, the recovery test of 5-FU was performed in human serum, and the recoveries of 95−105% of spiked 5-FU were obtained as shown in Table 2. These results indicated that the Mn-QDs as the probe was successful in time-resolved fluorescence detection of 5-FU in human serum. Various methods have been developed for the determination of 5-FU. Much research interest has been paid to the development and application of high-performance liquid chromatography (HPLC),[37] capillary electrophoresis (CE),[38a] and liquid chromatography/mass spectrometry (LC−MS).[38b] However, all these methods need to be deproteinized tediously from human serum sample before analysis, and even so, the LC or CE column usually suffered from losing the effectiveness because the column could be blocked by residual proteins in human serum sample. What is more, the harsh analytical conditions such as gradient elution and long analytical time (maybe more than 1 h)[37] were also necessary. Compared with the methods,[37,38] the time-resolved fluorometry was facile and rapid for the detection of 5-FU within 5 min because the troublesome sample pretreatment and gradient elution could be avoided.

CONCLUSIONS

In conclusion, a green and rapid microwave-assisted hydrothermal approach was successfully applied in the synthesis of Mn-QDs with high crystallinity, monodispersity, and good water solubility. The as-prepared Mn-QDs had strong and pure dopant PL, long fluorescence lifetime, and excellent photostability. A time-resolved fluorometry was established to determine 5-fluorouracil in human serum PBS solution using the Mn-QDs as fluorescence probe, which supported that the Mn-QDs were a new promising fluorescence probe for time-resolved fluorometry.

ASSOCIATED CONTENT

Supporting Information. XRD pattern of the Mn-doped ZnSe QDs with diffraction lines for cubic phases of bulk ZnSe shown for guidance (0.84% Mn/Zn ratio in the nanocrystals), EPR spectrum of the as-prepared Mn-doped ZnSe QDs, FT-IR spectrograms of the Mn-QDs capped with MPA, 5-FU, and the Mn-QDs/5-FU hybrids, possible mechanism of the quenching the emission of Mn-doped ZnSe QDs at 585 nm. This material is available free of charge via the Internet at http://pubs.acs.org.

AUTHOR INFORMATION

Corresponding Author

*E-mail: jrzhang@nju.edu.cn (J.Z.); jjzhu@nju.edu.cn (J.-J.Z.). Phone: +86 25 83686130. Fax: +86 25 83317761.

ACKNOWLEDGMENT

We gratefully appreciate the National Natural Science Foundation (20975048, 50972058, and 20805022) and the National Basic Research Program (2011CB933502) of China. This work was also supported by the China Postdoctoral Science Foundation (20100471294).

REFERENCES

(1) (a) Diamandis, E. P.; Christopoulos, T. K. *Anal. Chem.* **1990**, *62*, 1149A–1157A. (b) Dickson, E. F. G.; Pollak, A.; Diamandis, E. P. *Pharmacol. Ther.* **1995**, *66*, 207–235.

(2) (a) Ye, Z. Q.; Tan, M. Q.; Wang, G. L.; Yuan, J. L. *Anal. Chem.* **2004**, *76*, 513–518. (b) Nivriti, G.; Lawrence, W. M. *Cytometry* **2010**, *77A*, 1113.

(3) Seveus, L.; Väisälä, M.; Syrjänen, S.; Sandberg, M.; Kuusisto, A.; Harju, R.; Salo, J.; Hemmilä, I.; Kojola, H.; Soini, E. *Cytometry* **1992**, *13*, 329–338.

(4) Bruchez, M. J.; Moronne, M.; Gin, P.; Weiss, S.; Alivisatos, A. P. *Science* **1998**, *281*, 2013–2016.

(5) Chan, W. C. W.; Nile, S. *Science* **1998**, *281*, 2016–2018.

(6) Klimov, V. I.; Mikhailovsky, A. A.; Xu, S.; Malko, A.; Hollingsworth, J. A.; Leatherdale, C. A.; Eisler, H. J.; Bawendi, M. G. *Science* **2000**, *290*, 314–316.

(7) Wang, F.; Yu, H.; Jeong, S.; Pietryga, J. M.; Hollingsworth, J. A.; Gibbons, P. C.; Buhro, W. E. *ACS Nano* **2008**, *2*, 1903–1913.

(8) Peng, Z. A.; Peng, X. *J. Am. Chem. Soc.* **2001**, *123*, 183–184.

(9) Sun, J.; Wang, L.-W.; Buhro, W. E. *J. Am. Chem. Soc.* **2008**, *130*, 7997–8005.

(10) Hoshino, A.; Fujioka, K.; Oku, T.; Suga, M.; Sasaki, Y. F.; Ohta, T.; Yasuhara, M.; Suzuki, K.; Yamamoto, K. *Nano Lett.* **2004**, *4*, 2163–2169.

(11) Selvan, S. T.; Tan, T. T.; Ying, J. Y. *Adv. Mater.* **2005**, *17*, 1620–1625.

(12) Kirchner, C.; Liedl, T.; Kudera, S.; Pellegrino, T.; Javier, A. M.; Gaub, H. E.; Fertig, N.; Parak, W. J. *Nano Lett.* **2005**, *5*, 331–338.

(13) Cho, S. J.; Maysinger, D.; Jain, M.; Roder, B.; Hackbarth, S.; Winnik, F. M. *Langmuir* **2007**, *23*, 1974–1980.
(14) Pradhan, N.; Goorskey, D.; Thessing, J.; Peng, X. *J. Am. Chem. Soc.* **2005**, *127*, 17586–17587.
(15) Li, J. J.; Wang, Y. A.; Guo, W.; Keay, J. C.; Mishima, T. D.; Johnson, M. B.; Peng, X. *J. Am. Chem. Soc.* **2003**, *125*, 12567–12575.
(16) Empedocles, S. A.; Norris, D. J.; Bawendi, M. G. *Phys. Rev. Lett.* **1996**, *77*, 3873–3876.
(17) Bhargava, R. N.; Gallagher, D. *Phys. Rev. Lett.* **1994**, *72*, 416.
(18) Thakar, R.; Chen, Y. C.; Snee, P. T. *Nano Lett.* **2007**, *7*, 3429–3432.
(19) Xue, J.; Ye, Y.; Medina, F.; Martinez, L.; Lopez-Rivera, S. A.; Giriat, W. *J. Lumin.* **1998**, *78*, 173.
(20) (a) He, Y.; Wang, H. F.; Yan, X. P. *Anal. Chem.* **2008**, *80*, 3832–3837. (b) He, Y.; Wang, H. F.; Yan, X. P. *Chem.—Eur. J.* **2009**, *15*, 5436–5440. (c) Wang, H. F.; He, Y.; Ji, T. R.; Yan, X. P. *Anal. Chem.* **2009**, *81*, 1615–1621. (d) Wu, P.; He, Y.; Wang, H. F.; Yan, X. P. *Anal. Chem.* **2010**, *82*, 1427–1433. (e) Wang, H. F.; Li, Y.; Wu, Y. Y.; He, Y.; Yan, X. P. *Chem.—Eur. J.* **2010**, *16*, 12988–12994. (f) Zou, W. S.; Sheng, D.; Ge, X.; Qiao, J. Q.; Lian, H. Z. *Anal. Chem.* **2011**, *83*, 30–37. (g) Wu, P.; Miao, L. N.; Wang, H. F.; Shao, X. G.; Yan, X. P. *Angew. Chem., Int. Ed.* **2011**, *50*, 8118–8121.
(21) Quan, Z. W.; Wang, Z. L.; Yang, P. P.; Lin, J.; Fang, J. Y. *Inorg. Chem.* **2007**, *46*, 1354–1360.
(22) Yang, H.; Holloway, P. H. *Adv. Funct. Mater.* **2004**, *14*, 152.
(23) Narayan, P.; Peng, X. *J. Am. Chem. Soc.* **2007**, *129*, 3339–3347.
(24) Norris, D. J.; Yao, N.; Charnock, F. T.; Kennedy, T. A. *Nano Lett.* **2001**, *1*, 3–7.
(25) Pradhan, N.; Battaglia, D. M.; Liu, Y. C.; Peng, X. *Nano Lett.* **2007**, *7*, 312–317.
(26) Correa-Duarte, M. A.; Giersig, M.; Kotov, N. A.; Liz-Marzan, L. M. *Langmuir* **1998**, *14*, 6430–6435.
(27) Li, L.; Qian, H. F.; Ren, J. C. *Chem. Commun.* **2005**, 528–530.
(28) Bharat, L. N.; Johnson, O.; Sridhar, K. *J. Phys. Chem. B* **2001**, *105*, 8356–8360.
(29) Zhu, D.; Jiang, X.; Zhao, C.; Sun, X.; Zhang, J. R.; Zhu, J. J. *Chem. Commun.* **2010**, *46* (29), 5226–5228.
(30) Suyver, J. F.; Wuister, S. F.; Kelly, J. J.; Meijerink, A. *Phys. Chem. Chem. Phys.* **2000**, *2*, 5445.
(31) Gan, C. L.; Zhang, Y. P.; Xiao, M.; Battaglia, D.; Peng, X. G. *Appl. Phys. Lett.* **2008**, *92*, 241111.
(32) Demas, J. N.; Crosby, G. A. *J. Phys. Chem.* **1971**, *75*, 991.
(33) Klayman, D. L.; Griffin, T. S. *J. Am. Chem. Soc.* **1973**, *95*, 197–199.
(34) Brus, L. E. *J. Chem. Phys.* **1983**, *79*, 5566–5571.
(35) Lakowicz, J. R.; Gryczynski, I.; Gryczynski, Z.; Murphy, C. J. *J. Phys. Chem. B* **1999**, *103*, 7613.
(36) Michalet, X.; Pinaud, F. F.; Bentolila, L. A.; Tsay, J. M.; Doose, S.; Li, J. J.; Sandaresan, G.; Wu, A. M.; Gambhir, S. S.; Weiss, S. *Science* **2005**, *307*, 538.
(37) (a) Zambonin, C. G.; Aresta, A.; Grano, M. *J. Pharm. Biomed. Anal.* **1998**, *17*, 11–16. (b) Chu, D.; Gu, J.; Liu, W.; Fawcett, J. P.; Dong, Q. *J. Chromatogr., B* **2003**, *795*, 377–382.
(38) (a) Prochazkova, A.; Liu, S.; Friess, H.; Aebi, S.; Thormann, W. *J. Chromatogr., A* **2001**, *916*, 215–224. (b) Remaud, G.; Boisdron-Celle, M.; Morel, A.; Gamelin, A. *J. Chromatogr., B* **2005**, *824*, 153–160.